Title

THE LOWEST TRIPLET STATE OF SUBSTITUTED BENZENES: I. THE OPTICALLY DETECTED MAGNETIC RESONANCE

Authors

Buckley, M. J.
Harris, C.B.

Publication Date

1971-07-01

Submitted to
Journal of Chemical Physics

LBL-128
Preprint

THE LOWEST TRIPLET STATE OF SUBSTITUTED BENZENES: I. THE OPTICALLY DETECTED MAGNETIC RESONANCE

M. J. Buckley and C. B. Harris

July 1971

AEC Contract No. W-7405-eng-48

LAWRENCE RADIATION LABORATORY
UNIVERSITY of CALIFORNIA BERKELEY

DISCLAIMER

The Lowest Triplet State of Substituted Benzenes: I. The Optically Detected Magnetic Resonance of Paradichlorobenzene

by

M. J. Buckley and C. B. Harris†

The Department of Chemistry, University of California, and
the Inorganic Materials Research Division, Lawrence Berkeley Laboratory,
Berkeley, California 94720

ABSTRACT

The optically detected magnetic resonance (ODMR) of paradichlorobenzene in its first $^3\pi\pi^*$ state is reported. The structures of the three zero-field transitions are interpreted in terms of a Hamiltonian incorporating the electron spin-spin, chlorine nuclear quadrupole and chlorine hyperfine interactions. It is concluded from an analysis of the spin Hamiltonian parameters that the triplet spin density in the chlorine out-of-plane orbitals is small, the chlorine electric field gradient is significantly reduced in the $^3\pi\pi^*$ state as compared to the value for the ground state, and that the molecule most likely is distorted to a C_{2h} configuration.

† Alfred P. Sloan Fellow

I. Introduction

Optically detected magnetic resonance in phosphorescent triplet states has been an area of considerable interest.[1-3] Not only has it been utilized as a method for determining parameters generally accessible from conventional electron spin resonance, but it has also provided new techniques[4] for elucidating other phenomena associated with the triplet state, such a intra- and intermolecular energy transfer.[5-6] In addition, it has been used to determine the orbital symmetries of certain triplet states.[7-8] In this connection the first excited triplet state of benzene and substituted benzenes have been studied by both conventional spectroscopic techniques and phosphorescence microwave double resonance (PMDR) spectroscopy.[4] Although many features associated with the $\pi\pi^*$ triplet state of benzene such as its orbital symmetry and molecular geometry have been determined, the same is not true for many substituted benzenes. One particular molecule in this category which has been investigated by both standard optical spectroscopy[9] and PMDR techniques[10] is paradichlorobenzene (DCB). The conclusions for the two investigations differ. Castro and Hochstrasser,[9] on the basis of a high resolution triplet absorption spectrum have assigned the orbital symmetry of the first excited triplet state of DCB as $^3B_{2u}$. This is not the state derived from the accepted[11] assignment for the lowest triplet state in benzene, $^3B_{1u}$.

On the basis of the relationships between magnetic resonance parameters, the spin-orbit symmetries of the magnetic sublevels and the phosphorescence electric dipole activity as elucidated by optically detected magnetic

resonance (ODMR) in zero field, the lowest triplet DCB state has been alternatively assigned as $^3B_{1u}$.[8] A complete discussion of the orbital assignment and molecular structure of DCB will be presented in a later communication.[10] We wish to deal here with results that bear more directly upon the electron distribution in the $^3\pi\pi^*$ state of DCB as obtained from zero-field ODMR experiments. In this connection the importance of the sign of the zero-field parameter E will be discussed in connection with the orbital symmetry. The major emphasis of this investigation, however, will be addressed to answering questions such as: Do the chlorines participate significantly in delocalizing the electron spin in the DCB $^3\pi\pi^*$ state? Is DCB distorted, as suggested by Castro and Hochstrasser,[9] in the excited state? And is the electric field gradient tensor at the chlorines significantly changed upon excitation?

II. Experimental

A. Zero-Field Optically Detected Magnetic Resonance

The basic experimental arrangement is shown in Figure 1. The sample was mounted inside a microwave helical slow wave structure[12] attached to a rigid stainless steel coaxial line. The whole assembly was suspended in a liquid helium dewar. The light from a PEK 100-watt mercury short arc lamp was collimated and filtered by either an interference filter centered at 3100 Å or a combination of Corning glass and solution filters to obtain the desired excitation wavelength. The phosphorescence was collected at a 90 degree angle to the exciting source, focused through an appropriate Corning filter to remove scattered light and isolated by a Jarrell-Ash 3/4 meter Czerney-Turner spectrometer equipped with a cooled (-20°C) EMI 6256S photomultiplier. The cathode of the photomultiplier was held at a negative potential by a Fluke 415B power supply while the anode of the photomultiplier was connected to a Keithly model 610 CR electrometer through an adjustable load resistor. The electrometer was finally connected to the signal channel of a PAR model HR-8 lock-in amplifier.

The microwave field was supplied by a Hewlett-Packard sweep oscillator model 8690B equipped with plug-in units to cover the appropriate range. Its output was connected to a broad band 1 watt traveling wave tube amplifier which was then fed consecutively through a directional coupler, a band-pass filter and an isolator and finally terminated on a rigid 50 Ω coaxial line to which the helix was mounted. The signal required to

amplitude modulate the microwave sweep oscillator was supplied by a Hewlett-Packard model 211 AR square wave generator which was also connected to the reference channel of the lock-in amplifier. The output of the lock-in amplifier drove the Y axis of a Hewlett-Packard model 7004B X-Y recorder while the X-axis was driven by the ramp voltage from the microwave sweep oscillator.

The zero-field ESR experiments were performed by monitoring the change in phosphorescence intensity of the sample while varying the frequency of the modulated microwave field. The majority of the ESR spectra were obtained by square wave amplitude modulation with a frequency of 10 to 20 Hz and a modulation depth of $\geq$ 25 db. The microwave oscillator sweep circuit was modified by the addition of an assembly which permitted switching between external capacitors. With this arrangement sweep times as long as several thousand seconds were possible permitting the use of sweep rates as low as 0.025 MHz/sec. In this manner advantage could be taken of the long time constants (30-100 sec) available in the lock-in amplifier. The amplitude of the microwave field was adjusted when necessary by precision attenuators inserted at the output of the sweep generator.

B. Zero-Field Optically Detected ENDOR

The experimental arrangement normally employed for optically detected ENDOR along with an enlarged view of the sample, helix and ENDOR coils is illustrated in Figure 2. The optical and microwave equipment used in the ENDOR experiments was the same as that used in the ESR experiment

except for the addition of a radiofrequency field. This was supplied by a Hewlett-Packard model 8601A sweep oscillator that covers the region from 0.1 to 110 MHz. The rf sweep oscillator was modified by use of an external timing capacitor to permit sweep times as long as 2000 seconds. Its output was amplitude modulated by an E G & G model LG101/N linear gate. The gate was driven by the square wave generator which also served as the reference signal for the lock-in amplifier. The rf was then amplified consecutively by two broad-band distributed amplifiers, a four watt unit and a 20 watt unit and connected to the ENDOR coils. These amplifiers have the advantage that they operate over the range of 1 to 50 MHz without the need of adjustment.

The ENDOR coil consists of a "bridge T" constant resistance network in a Helmholtz arrangement. This design has the advantage of appearing resistive (50 Ω) at its input for frequencies from 1 to 50 MHz. This permits rf fields to be applied to the sample over this frequency range without adjustment.

The ENDOR experiments were usually performed by saturating an ESR transition with the microwave field while varying the frequency of the rf field. Either the microwave or rf field may be modulated; however, it was usually preferable to modulate the latter since in this case only the changes in the phosphorescence intensity due to the ENDOR resonances are detected with the lock-in amplifier. On the other hand, if the microwave field is modulated, there is a constant signal due to the ESR transition which changes in intensity when the rf field is swept through resonance.

A useful modification of the ENDOR experiment is to simultaneously saturate an ENDOR transition and sweep the microwave field. In this case, only the electron spin transitions that have energy levels in common with the nuclear levels coupled by the rf field are detected. An advantage of this technique is that the structure of the ESR transition can be simplified since the contributions to the spectrum from different isotopes and/or nuclei may be isolated.

It is interesting to note that if both an ESR and ENDOR transition are saturated while modulating the rf field and the phosphorescence spectrum is scanned, it is possible to isolate the contribution to the phosphorescence spectrum from molecules containing different nuclear isotopes. As an example, if the phosphorescence from a molecule such as chlorobenzene is monitored and a ^{35}Cl ENDOR transition is detected while modulating the rf field, only the contribution to the phosphorescence spectrum from molecules containing the ^{35}Cl isotope will be detected. The same experiment may then be repeated detecting only the contribution from the molecules containing the ^{37}Cl isotope.

The measurement of the ^{35}Cl pure nuclear quadrupole resonance of ground state DCB at 4.2°K was achieved with the use of a marginal oscillator described by Fayer and Harris.[12] The sample coil was extended by placing the leads to the coil inside a section of stainless steel tubing bent at a right angle in order to support the coil in a liquid helium dewar. The dewar used in this experiment was constructed by inserting a small narrow mouth commercial dewar inside a larger wide mouth dewar. The outer dewar was filled with liquid nitrogen and the inner dewar with liquid helium.

This arrangement held helium for about 30 minutes with the sample in place. Zeeman modulation was achieved by use of a selenoid wound around the outer dewar.

C. Sample

Eastman Organic paradichlorobenzene was degassed and zone refined for 100 passes at two inches/hour. Single crystals of DCB grown by the Bridgeman technique were mounted inside the helical slow wave structure [13] and irradiated through the helical windings with near uv light. The temperature of the sample was usually lowered to approximately 1.3°K by pumping on the liquid helium with three Kinney model KTC-21 vaucum pumps operated in parallel.

III. Results

A. The Optically Detected ESR Spectra

The ODMR spectra of DCB in zero magnetic field have been observed while monitoring the emission from two distinct traps. Although the zero-field parameters are reported for both traps (Cf. Table 2) only the ODMR spectra due to the shallow trap (labeled x) will be discussed. The chlorine nuclear quadrupole and hyperfine structure of the ODMR spectra observed for the deep trap are essentially the same as those for the shallow trap; however, the zero-field values are about 5% lower.

The observed ODMR spectra of DCB are due to the interaction of three isotopically distinct molecular species. The fractional natural abundances of the ^{35}Cl and ^{37}Cl isotopes are approximately 3/4 and 1/4 respectively. Since there are two chlorine nuclei per molecule, the fractional distribution of the molecular species are:

$$\text{I} \qquad {}^{35}Cl - {}^{35}Cl = 9/16$$

$$\text{II} \qquad {}^{35}Cl - {}^{37}Cl = 6/16$$

$$\text{III} \qquad {}^{37}Cl - {}^{37}Cl = 1/16 .$$

The spectra obtained will therefore be treated as a superposition of the ODMR spectra due to each of the three molecular species.

The $\tau_x \rightarrow \tau_y$ (high frequency) transitions observed using amplitude modulation is shown in Figure 3. The remaining two electron spin transitions ($\tau_x \rightarrow \tau_z$ and $\tau_z \rightarrow \tau_y$) have essentially the same structure as the spectra

illustrated for the $\tau_x \rightarrow \tau_y$ transition; however, the signal-to-noise ratio of the $\tau_z \rightarrow \tau_y$ transition was substantially lower.

In Table 1 the possible ESR transitions involving the triplet electrons and one or more chlorine nuclei are listed as to type (A,B,C, D,E, or F) and the molecular species (I,II or III) which can undergo each type of transition. The intensity of the transitions involving the electron and one chlorine spin (B and C) and those involving the electron and two chlorine spins (D, E and F) must be considered separately. The ratio of the intensities of the transitions involving a single ^{35}Cl spin (type B) to those involving a single ^{37}Cl spin (type C) should be three to one on the basis of the ratio of ^{35}Cl to ^{37}Cl. The ratio of the intensities of the transitions involving two chlorine spins is likewise $I_D:I_E:I_F = 9:6:1$.

The structure of the $\tau_x \rightarrow \tau_y$ electron spin multiplet shown in Figure 3 is labeled according to the classification given in Table 1. Since the nuclear quadrupole moment of ^{35}Cl is larger than that of ^{37}Cl the outer pair of the four strong satellites are assigned as type B (^{35}Cl) and the inner pair as type C transitions (^{37}Cl). As can be seen, the ratio of the intensity of the transitions labeled B and C is approximately 3:1 as predicted. The ratio of the outermost satellites in Figure 3 are assigned to simultaneous double chlorine transitions (labeled D and E on the spectra). The intensity of these transitions is also approximately in the predicted ratio of 9:6. The transitions corresponding to simultaneous double ^{37}Cl transitions (type F) are not observed consistent with the small natural abundance of the molecular species responsible for these transitions. The inner pair of satellites

(labeled E in Figure 3) may be considered as simultaneous electron and ^{35}Cl and ^{37}Cl transitions. The higher frequency satellite represents a simultaneous electron spin transition, a ^{35}Cl ($\pm \frac{3}{2} \rightarrow \pm \frac{1}{2}$) and a ^{37}Cl ($\pm \frac{1}{2} \rightarrow \pm \frac{3}{2}$) transition while the lower frequency satellite represents the opposite chlorine transitions. These transitions are thus separated by the difference between the ^{35}Cl and ^{37}Cl nuclear quadrupole coupling constants. Naturally these occur for only those molecules that have one ^{35}Cl and one ^{37}Cl isotope. Since the matrix elements for these double chlorine transitions are of a different form than those associated with the other double chlorine transitions, the intensity of the inner satellites labeled E in Figure 3 may not be compared directly with the intensity of the outer satellites labeled D and F.

All transitions involving both an electron and a nuclear spin required several orders of magnitude greater microwave power to obtain intensities comparable to the electron only (type A) transition.

B. Optically Detected ENDOR

Chlorine ENDOR transitions were observed by saturating the ESR transitions associated with the $\tau_x \rightarrow \tau_y$ or $\tau_x \rightarrow \tau_z$ manifolds. Both the ^{35}Cl and ^{37}Cl ENDOR resonances were observed while saturating either ESR transition. Figures 4a and 4b illustrate the ^{35}Cl ENDOR resonances associated with the $\tau_x \rightarrow \tau_y$ and $\tau_x \rightarrow \tau_z$ transitions respectively.

As an extension of the ENDOR experiments a ^{35}Cl ENDOR transition was saturated while sweeping the $\tau_x \rightarrow \tau_z$ microwave transition. Since only the ENDOR time dependent magnetic field was amplitude modulated and

the change in phosphorescence intensity detected with a lock-in amplifier only the ESR transitions that involve at least one ^{35}Cl spin transition were detected. The spectrum obtained from this experiment is shown in Figure 5. As would be expected, satellites assigned as simultaneous electron and ^{37}Cl spin transitions (labeled C in Figure 3 are not observed.

All measured frequencies associated with the three electron spin zero-field transitions are given in Table 3, while the ^{35}Cl and ^{37}Cl ENDOR transitions are listed separately in Table 4.

C. Ground State ^{35}Cl NQR at 4.2°K

The pure ^{35}Cl nuclear quadrupole resonance spectra of DCB in its ground state is shown in Figure 6. Due to the long spin-lattice relaxation time it was difficult to avoid saturation and consequently the signal strength is reduced compared to that obtained at room temperature. In order to improve the signal-to-noise ratio, a large Zeeman field was used to modulate the sample which also produced a distorted lineshape.

IV. Discussion

A. The Spin Hamiltonian

The spectra may be satisfactorily explained in terms of a Hamiltonian of the form

$$H = H_{SS} + \sum_i H_Q + \sum_i H_{HF} \qquad (1)$$

where the summation is over the chlorine nuclei. The electron spin-spin Hamiltonian, H_{SS}, the chlorine nuclear quadrupole Hamiltonian, H_Q, and the chlorine nuclear-electron hyperfine Hamiltonian, H_{HF}, are given by:

$$H_{SS} = -XS_x^2 - YS_y^2 - ZS_z^2 , \qquad (2a)$$

$$H_Q = \frac{e^2qQ}{12}(3I_z^2 - 15/4) , \qquad (2b)$$

and

$$H_{HF} = A_{xx}S_xI_x , \qquad (2c)$$

with the axis system defined as x, out-of-plane; z, along the C-Cl bond direction; and y, the short in-plane axis.

Several assumptions have been made in writing the spin Hamiltonian in this form. Since these experiments were performed in the absence of an external magnetic field, no information is obtained from the ESR spectra as to the relative orientation of H_{SS}, H_Q and H_{HF}. The H_{SS} axis system is constrained by symmetry in D_{2h} to be along the molecular axis system. If the symmetry of DCB is less than D_{2h} then this restriction is not valid. However from analysis of the phosphorescence spectra, DCB has been found to reflect essentially D_{2h} symmetry although it is likely to be slightly

distorted in the excited state.[9,10] The orientation of H_Q in the ground state of DCB has been determined from Zeeman studies of the chlorine pure nuclear quadrupole resonance.[14] The principal axis of H_Q is within one degree of the C-Cl bond direction as determined from x-ray studies.[15]

In addition a small deviation of the principal axis of H_Q from this orientation would only produce a small error in the measured value of e^2qQ. This is because the coupling of H_Q and H_{SS} is through H_{HF} and (as is the case here) if H_{HF} is much less than e^2qQ the error introduced by assuming that the principal axis of H_Q is along the molecular axis is small.

The assumption that H_{HF} is coincident with H_{SS} and H_Q is the least satisfactory. However since it was only necessary to include the A_{xx} element of H_{HF} and since H_{HF} is an off-diagonal term in the spin Hamiltonian in zero field, a small deviation of A_{xx} from the x axis will only produce a small error in the magnitude of A_{xx}.

In addition the chlorine nuclear quadrupole asymmetry parameter has been neglected since its value is small in the ground state (.04) [14] and because it is only a small off-diagonal term in the spin Hamiltonian which could not be experimentally determined.

Furthermore the hyperfine interaction due to the four protons has been omitted. This is justified on the basis of the small proton hyperfine contribution to the ESR linewidth in zero field reported by Hutchison et al.[16] for the $^3\pi\pi^*$ state of naphthalene. The magnitude of this contribution is far smaller than the observed linewidths for DCB.

The choice of basis states used in calculating the spin Hamiltonian and the effect of H_Q and H_{HF} on the transition frequencies and intensities in zero field have been treated in detail in an earlier publication and will not be repeated here.[17]

Since the total spin of the system is integral we do not have the simplification of a Kramers degeneracy; consequently all 48 nuclear-electron spin states must be considered. The ODMR spectra were simulated by use of a computer program that diagonalized the spin Hamiltonian and calculated the transition frequencies and intensities. The spectra were calculated for only the ^{35}Cl-^{35}Cl species of DCB. After the best fit to these transitions was obtained, the nuclear quadrupole coupling constant of ^{35}Cl was multiplied by the ratio of the ^{37}Cl nuclear quadrupole moment to the ^{35}Cl nuclear quadrupole moment (0.78815)[18] in order to obtain the ^{37}Cl nuclear quadrupole coupling constant. The ^{37}Cl hyperfine interaction was obtained in a similar fashion by multiplying the ^{35}Cl hyperfine interaction (A_{xx}) by the ratio of $\gamma_{^{37}Cl}$ to $\gamma_{^{35}Cl}$ (0.8322). The spin Hamiltonian parameters used in simulating the spectra observed while monitoring the x-trap emission are listed in Table 2 along with the approximate values of H_{SS} for the y trap and the values reported for benzene.[19] The best value obtained for the ^{35}Cl nuclear quadrupole coupling constant was -64.50 MHz (^{37}Cl = -50.84 MHz) and for the ^{35}Cl hyperfine interaction A_{xx} = 22 MHz (^{37}Cl: A_{xx} = 18.3 MHz). The experimental and calculated ESR frequencies for the x trap of DCB are listed in Table 3. With the parameters used in the spin Hamiltonian all of the calculated transition frequencies are within experimental error. However, a small error in the calculated

frequencies is introduced since a weighted average of the transitions corresponding to a particular type was made.

The observed and calculated chlorine ENDOR transitions associated with the $\tau_x \rightarrow \tau_y$ and $\tau_x \rightarrow \tau_z$ multiplets are listed in Table 4. In addition to the linewidth of the ENDOR transitions, the large rf fields used in the ENDOR experiments (approximately twenty watts) makes the proper weighting of the calculated ENDOR frequencies unknown. Therefore only the range of calculated ENDOR frequencies is listed in Table 4.

B. Interpretation of the Spin Hamiltonian Parameters

Since both the triplet electron dipole-dipole interaction and spin-orbit coupling between the triplet and singlet states give a Hamiltonian of the same form as in Equation (2a), it is not possible from analysis of the ESR spectra to separate the two contributions. However as previously discussed[17] it is reasonable to assume that the spin-orbit contribution accounts for less than 5% of the measured splitting in DCB and therefore will be neglected in the following discussion.

From previous experimental[20,21] and theoretical[22-25] studies of aromatic molecules in $\pi\pi^*$ triplet states it is almost certain that in DCB the largest component of the electron spin-spin tensor in its principal axis system is along the molecular axis normal to the plane (x). Indeed this is what is observed for the lowest $\pi\pi^*$ triplet state of benzene.[19] The ordering of the interaction along the two in-plane molecular axes is however not immediately apparent. From the analysis of the spectra of DCB utilizing

phosphorescence microwave double resonance spectroscopy the component of the electron spin-spin interaction along the molecular y (or short in-plane axis) has been assigned as the larger of the two in-plane components of the electron spin-spin tensor.[8]

Since the zero-field splitting parameters D and D* $\left(D^* = (D^2 + 3E^2)^{\frac{1}{2}}\right)$ are primarily a function of the size of the π system involved in the excitation,[26] the value of these parameters for both DCB and benzene should be similar if DCB is a $\pi\pi^*$ triplet. As can be seen in Table 2 the values of D and D* for both traps of DCB differ from the corresponding values for benzene by only a few percent which is strong confirmation of the assignment of the excited triplet state of DCB as a $\pi\pi^*$ state. The zero-field splitting parameter E which is a measure of the anisotropy of the triplet electron distribution in the molecular plane is, however, quite different for both molecules. If the benzene molecule possessed D_{6h} symmetry in the excited state, E must be zero by symmetry. The finite value of E for benzene has been explained by de Groot and van der Waals[19,27] on the basis of a distortion of the benzene ring from the D_{6h} to D_{2h}.

A quantitative analysis of the E value of DCB is difficult since accurate wavefunctions are not available for the chlorines. However from a simple consideration of the perturbation of the triplet electron distribution in benzene due to the addition of two para-chlorines, it is expected that the τ_z level will be lowered and the τ_y level raised in energy. Since the E value of DCB is larger than the E value of benzene, this model predicts that in DCB the τ_y level is higher in energy than the τ_z level. This of course gives the opposite sign of E for DCB as compared

to benzene, and is consistent with the ordering of the triplet energy levels previously obtained from analysis of the phosphorescence microwave double resonance spectra.

It is interesting to note that in 1,2,4,5 tetrachlorobenzene (TCB) the inclusion of chlorine interactions would predict the τ_z level to be higher in energy than the τ_y level; consequently, the E value would have the same sign as benzene. Other substituted chlorobenzenes should have E values between DCB and TCB.

The importance of the zero-field splitting of DCB and TCB is that the presence of the chlorines acting as perturbations on the excited state of benzene raises the possibility that the symmetry of the excited state of DCB and TCB is different than that of the excited state of benzene. As has been discussed[8] the sign of E in part answers this interesting question.

The absolute value of the chlorine nuclear quadrupole coupling constant (e^2qQ) in the excited state of DCB is significantly reduced compared to the corresponding value for the ground state.

With the assumption that the asymmetry parameter (η)may be neglected, the value of e^2qQ for the ^{35}Cl nuclei of DCB in its excited triplet state at 1.3°K is -64.5 MHz. The measured pure nuclear quadrupole resonance frequency of DCB in its ground state at 4.2°K is 34.831 MHz which, if η is assumed to equal zero, corresponds to a value of e^2qQ of -69.662 MHz. The assumption that η may be neglected is justified on the basis that e^2qQ is not changed significantly for small values of η and for the ground state of DCB at room temperature η is only 0.08.[14] Indeed, from

the explicit dependence of e^2qQ on η as illustrated in Figure 7, the assumption that e^2qQ is simply twice the pure NQR transition frequency causes a positive error in e^2qQ of less than 5% for $\eta \leq 0.5$. The sign of e^2qQ is not obtained from either the measurement of the pure NQR transition frequency or the spin Hamiltonian; however, from other theoretical and experimental studies e^2qQ for Cl is known to be negative for covalently bonded compounds.[28]

The increase of 52 KHz in the pure NQR frequency of the ground state of DCB upon lowering the temperature of the sample from 77°K (ν = 34.779 MHz) to 4.2°K (ν = 34.831 MHz) is consistent with Bayer's theory[29] which treats the temperature dependence of the NQR frequency in terms of the molecular torsional motions. More important, however, is the fact that the small change in the pure NQR transition frequency indicates that there is no major physical change in the environment of the chlorine nuclei in DCB upon cooling. Therefore, the difference in e^2qQ between the ground and excited states of DCB is clearly due to a change in the electric field gradient (q) at the chlorines upon excitation. The magnitude of the decrease in the absolute value of e^2qQ upon excitation is interesting because: a) the absolute value of e^2qQ in the triplet state of DCB is significantly less than the value reported for the ground state of <u>any</u> chlorine bonded to an aromatic molecule;[30] and b) the decrease in $|e^2qQ|$ upon excitation to the lowest $^3\pi\pi^*$ state of 8-chloroquinoline[31] and 1,2,4,5 tetrachlorobenzene[32] is far less than the decrease in $|e^2qQ|$ for DCB.

In contrast to the electron spin-spin and hyperfine interactions which are a function of only the triplet electrons, e^2qQ is dependent

upon the distribution of all electrons. Since electrons in s orbitals have spherical symmetry, they do not contribute to the field gradient. A closed p shell also contributes nothing to the field gradient, and therefore following the analysis of Bersohn[33] the field gradient in DCB can be considered as arising from a hole in the chlorine p_z orbital and a partial hole in the chlorine p_x orbital. The total contribution is due to two axially symmetric tensors whose major axes are perpendicular. In Table 5 the contributions to the field gradient are expressed in terms of the number of holes in the p_x and p_z chlorine orbitals.

The difference in e^2qQ for the excited and ground state may be written,

$$\Delta e^2qQ = e^2(q_T - q_G)Q \qquad (3)$$

where q_T and q_G refer to the field gradient at the chlorines in the triplet and ground states of DCB respectively. Equation 3 may be expressed in terms of the number of holes in the p_z and p_x orbitals as

$$\Delta e^2qQ = e[\sigma_T-\sigma_G] - \tfrac{1}{2}[\delta_T-\delta_G]Q \qquad (4)$$

Since Δe^2qQ is negative, one of the following conditions must be met: a) $\sigma_G > \sigma_T$, or b) $\delta_T > \delta_G$. If σ_G is greater than σ_T, the number of holes has decreased along the carbon-chlorine bond, and therefore the chlorine nuclei are more successful in competing for electrons in the excited state. However since the sigma electrons are not involved in the excitation, this effect should be very small. If δ_T is greater than δ_G, the out-of-plane chlorine p_x orbital has lost electrons. An increase

in the number of holes in the p_x orbital would be the most likely explanation of the decrease in e^2qQ since the chlorine p_x orbitals are allowed by symmetry to interact with the carbon p_x orbitals. The increase in the number of holes in the chlorine p_x orbital can come about from either an increase in the double bond character of the C-Cl bond or a "bent" C-Cl bond. Bray, Barnes and Bersohn[30] have shown that although the overlap of the carbon and chlorine p_x orbitals is reduced with a bent C-Cl bond, the chlorine p_x orbitals may overlap with the sigma system, consequently increasing the number of holes in the p_x orbital of chlorine (δ_T) relative to the number of holes in the p_x orbital in the ground state (δ_G).

Although it is not possible a priori to distinguish between these two possibilities the interpretation of the change in e^2qQ as arising from a bent C-Cl bond is reasonable in view of other experimental results.

The phosphorescence of DCB to the origin is from all three triplet levels which requires that DCB have less than D_{2h} symmetry in its $^3\pi\pi^*$ state. In addition the strongest vibronic progression in the phosphorescence spectra (b_{2g}) corresponds to a trans C-Cl bending motion which clearly indicates that this is most significant mode of distortion. Finally the measured value of the out-of-plane chlorine hyperfine interaction for the $^3\pi\pi^*$ state of 8-chloroquinoline (15 MHz) is approximately the same as that observed for the $^3\pi\pi^*$ state of DCB (22 MHz). However in 8-chloroquinoline the chlorine nuclear quadrupole coupling constant is essentially unchanged upon excitation. In view of these observations it seems reasonable to interpret the change in e^2qQ as arising from a bent C-Cl bond.

In summary it appears that the chlorines do significantly influence the in-plane distribution of the triplet electrons. In fact the position of the chlorines is most likely the major factor in determining the sign and magnitude of the zero-field splitting parameter E. A distortion of DCB is consistent with the parameters obtained from the spin Hamiltonian and the phosphorescence spectra supporting the hypothesis that the symmetry of DCB is reduced from D_{2h} to C_{2h} in its $^3\pi\pi^*$ state due to a trans C-Cl bent bond.

Acknowledgements

This work was supported by the Inorganic Materials Research Division of the Lawrence Berkeley Laboratory under the auspices of the U.S. Atomic Energy Commission.

Table 1

ESR Transitions in Paradichlorobenzene

Transition Type	Simultaneous Transitions	Molecular Species
A	Electron Spin	I, II, III
B	Electron and ^{35}Cl Spins	I, II
C	Electron and ^{37}Cl Spins	II, III
D	Electron, ^{35}Cl and ^{35}Cl Spins	I
E	Electron, ^{35}Cl and ^{37}Cl Spins	II
F	Electron, ^{37}Cl and ^{37}Cl Spins	III

Table 2

Zero-Field Splitting Parameters (MHz)

	Paradichlorobenzene *		Benzene† -h_4
	X Trap (1.3°K)	Y Trap (4.2°K)	In Benzene-d_6 (1.95°K)
X	-2988.75	-2967.7	-3159.8
Z	616.07	654.4	1769.4
Y	2372.68	2313.4	1385.0
D‡	4483.13	4451.6	4739.7
E‡	-878.31	-829.5	+192.2
D*	4733.8	4677.7	4793.2
e^2qQ	-64.5	-	-
$A_{zz}(^{35}Cl)$	22	-	-

‡ In order to be consistent with the standard ESR definitions we have defined

$$D = -3/2\ X \quad \text{and} \quad E = 1/2\ (Z-Y)$$

† Data from reference 19 expressed in our axis system.

* Phosphorescence origin: X trap (27868 cm^{-1}) and Y trap (27807 cm^{-1}).

Table 3

Measured and Calculated ESR Transitions of the $^3\pi\pi^*$ State of Paradichlorobenzene (X Trap)

	Measured Frequency (MHz)	σ	Calculated Frequency	Classification
a) $\tau_x \rightarrow \tau_y$				
	5426.7	1.0*	5426.91	D
	5419.6	1.0*	5419.56	E
	5394.56	0.41	5394.62	B
	5387.86	0.41	5387.79	C
	5368.73	0.64	5368.89	E
	5362.20	0.34	5362.14	A
	5355.13	0.25	5355.12	E
	5336.67	0.24	5366.50	C
	5329.74	0.28	5329.75	B
	5303.8	1.0*	5304.11	E
	5296.5	1.0*	5297.35	D
b) $\tau_x \rightarrow \tau_z$	3636.03	.07	3636.13	B
	3629.65	.18	3629.56	C
	3611.18	.24	3611.04	E
	3604.19	.25	3604.10	A
	3597.69	.31	3597.43	E
	3578.90	.22	3578.89	C
	3571.88	.34	3571.99	B
c) $\tau_z \rightarrow \tau_y$	1791.1	1.5	1791.13	B
	1758.2	1.0	1758.05	A
	1724.5	1.5	1726.55	B

* Estimated value of σ

Table 4

Measured and Calculated Chlorine ENDOR Transitions of the $^3\pi\pi^*$ State of Paradichlorobenzene (X Trap)

	Measured Frequency in MHz (±.05)	Calculated Frequency in MHz (range)
	$\tau_x \rightarrow \tau_y$ Manifold	
^{35}Cl	32.06; 32.96	31.56 - 33.03
^{37}Cl	25.12; 26.00	24.94 - 26.09
	$\tau_x \rightarrow \tau_z$ Manifold	
^{35}Cl	31.75; 33.13	31.53 - 32.94
^{37}Cl	24.94; 26.19	24.79 - 25.90

Table 5

Contributions to the Chlorine Nuclear Quadrupole Coupline Constant

Chlorine Orbital	No. of Holes	Contribution to V_{xx}	V_{yy}	V_{zz}
P_x	δ	δq	$-\delta q/2$	$-\delta q/2$
P_z	σ	$-\sigma q/2$	$-\sigma q/2$	σq

Total Contribution

$$V_{xx} = (\delta - \sigma/2)q$$

$$V_{yy} = -1/2(\delta + \sigma)q$$

$$V_{zz} = (\sigma - \delta/2)q$$

References

1. M. Sharnoff, J. Chem. Phys. 46, 3263 (1967); J. Schmidt and J. H. van der Waals, Chem. Phys. Letters 2, 640 (1968).
2. C. B. Harris, D. S. Tinti, M. A. El-Sayed and A. H. Maki, Chem. Phys. Letters 4, 409 (1969).
3. A. L. Kwiram, Chem. Phys. Letters 1, 272 (1967).
4. D. S. Tinti, M. A. El-Sayed, A. H. Maki and C. B. Harris, Chem. Phys. Letters 3, 343 (1969).
5. D. S. Tinti and M. A. El-Sayed, J. Chem. Phys. 54, 2529 (1971).
6. A. H. Francis and C. B. Harris, Chem. Phys. Letters 9, 188 (1971).
7. A. A. Gwaiz, M. A. El-Sayed and D. S. Tinti, Chem. Phys. Letters 9, 454 (1971).
8. M. J. Buckley, C. B. Harris and R. M. Panos, J. Am. Chem. Soc. XX, XXX (1971).
9. G. Castro and R. M. Hochstrasser, J. Chem. Phys. 46, 3617 (1967).
10. M. J. Buckley, C. B. Harris and R. M. Panos, unpublished results.
11. R. R. Gilman and J. De Heer, J. Chem. Phys. 52, 4287 (1969).
12. M. D. Fayer and C. B. Harris, Inorg. Chem. 8, 2792 (1969).
13. R. H. Webb, Rev. Sci. Instr. 33, 732 (1962).
14. C. Dean, Thesis, Harvard University (1952).
15. E. Frasson, C. Garbuquo and S. Bezzi, Acta Cryst. 12, 126 (1959).
16. C. A. Hutchison, Jr., J. V. Nicholas and G. W. Scott, J. Chem. Phys. 53, 1906 (1970).
17. M. J. Buckley and C. B. Harris, J. Phys. Chem. XX, XXX (1971).
18. C. H. Townes, Handbuch der Physik, edited by S. Flugge (Springer Verlag, Berlin, 1958), Vol. 38, p. 444.

19. M. S. De Groot, I. A. M. Hesselman and J. H. van der Waals, Mol. Phys. 16, 45 (1969).

20. C. A. Hutchison, Jr. and B. W. Mangum, J. Chem. Phys. 34, 908 (1961).

21. N. Hirota, C. A. Hutchison, Jr., and P. Palmer, J. Chem. Phys. 40, 3717 (1964).

22. M. Gouterman and W. Moffitt, J. Chem. Phys. 30, 1107 (1959).

23. M. Gouterman, J. Chem. Phys. 30, 1369 (1959).

24. H. Hamika, J. Chem. Phys. 31, 815 (1963).

25. M. Godfrey, C. W. Kern and M. Karplus, J. Chem. Phys. 44, 4459 (1966).

26. A. Carrington and A. D. McLachlan, Introduction to Magnetic Resonance, (Harper and Row, 1967), p. 125-126.

27. M. S. De Groot and J. H. van der Waals, Mol. Phys. 6, 545 (1963).

28. C. H. Townes and A. L. Schawlow, Microwave Spectroscopy (McGraw-Hill, N. Y., 1955), chapter 9.

29. H. Bayer, Z. Physik, 130, 227 (1951).

30. P. J. Bray, R. G. Barnes and R. Bersohn, J. Chem. Phys. 25, 813 (1956).

31. M. J. Buckley and C. B. Harris, Chem. Phys. Letters 5, 205 (1970).

32. A. H. Francis and C. B. Harris, unpublished results.

33. R. Bersohn, J. Chem. Phys. 22, 2078 (1954).

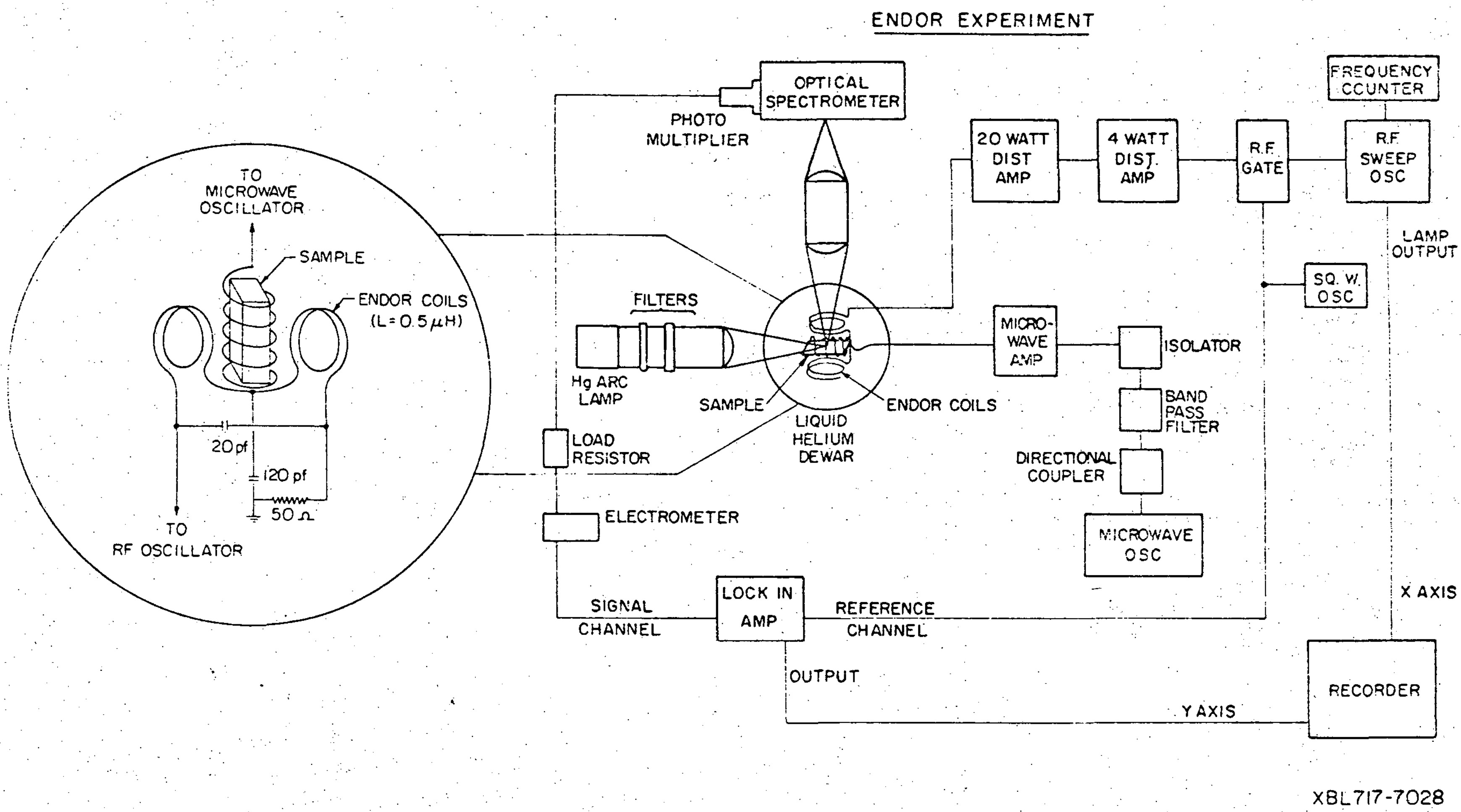
ENDOR EXPERIMENT
OPTICAL SPECTROMETER
PHOTO MULTIPLIER
FREQUENCY COUNTER
20 WATT DIST AMP
4 WATT DIST. AMP
R.F. GATE
R.F. SWEEP OSC
LAMP OUTPUT
SQ. W. OSC
TO MICROWAVE OSCILLATOR
SAMPLE
ENDOR COILS (L=0.5μH)
20pf
120 pf
50Ω
TO RF OSCILLATOR
FILTERS
Hg ARC LAMP
SAMPLE
LIQUID HELIUM DEWAR
ENDOR COILS
MICRO-WAVE AMP
ISOLATOR
BAND PASS FILTER
DIRECTIONAL COUPLER
MICROWAVE OSC
LOAD RESISTOR
ELECTROMETER
SIGNAL CHANNEL
LOCK IN AMP
REFERENCE CHANNEL
OUTPUT
Y AXIS
X AXIS
RECORDER
XBL717-7028

Fig. 2

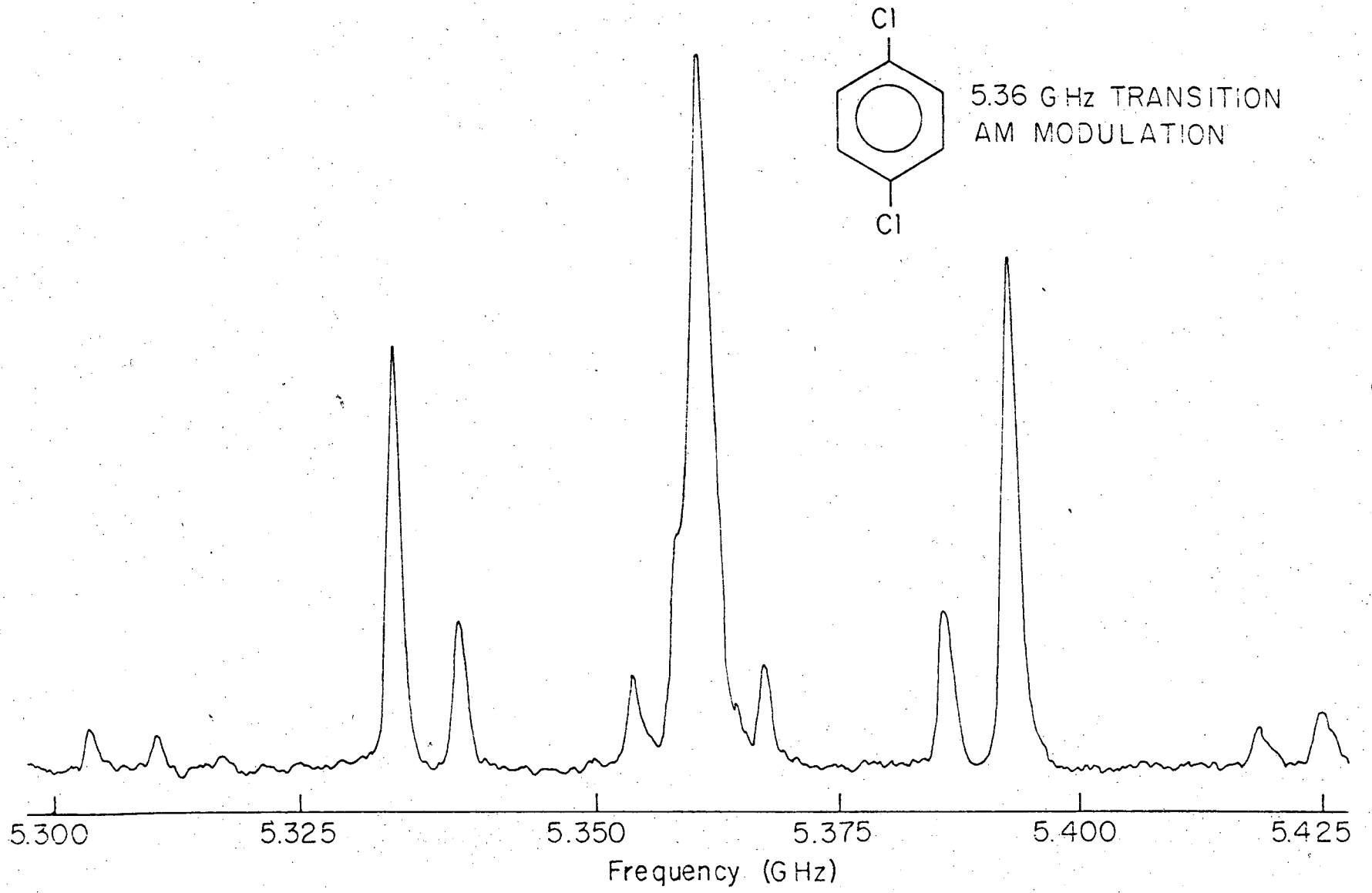
Cl
Cl
5.36 GHz TRANSITION
AM MODULATION
5.300
5.325
5.350
5.375
5.400
5.425
Frequency (GHz)

Fig. 3

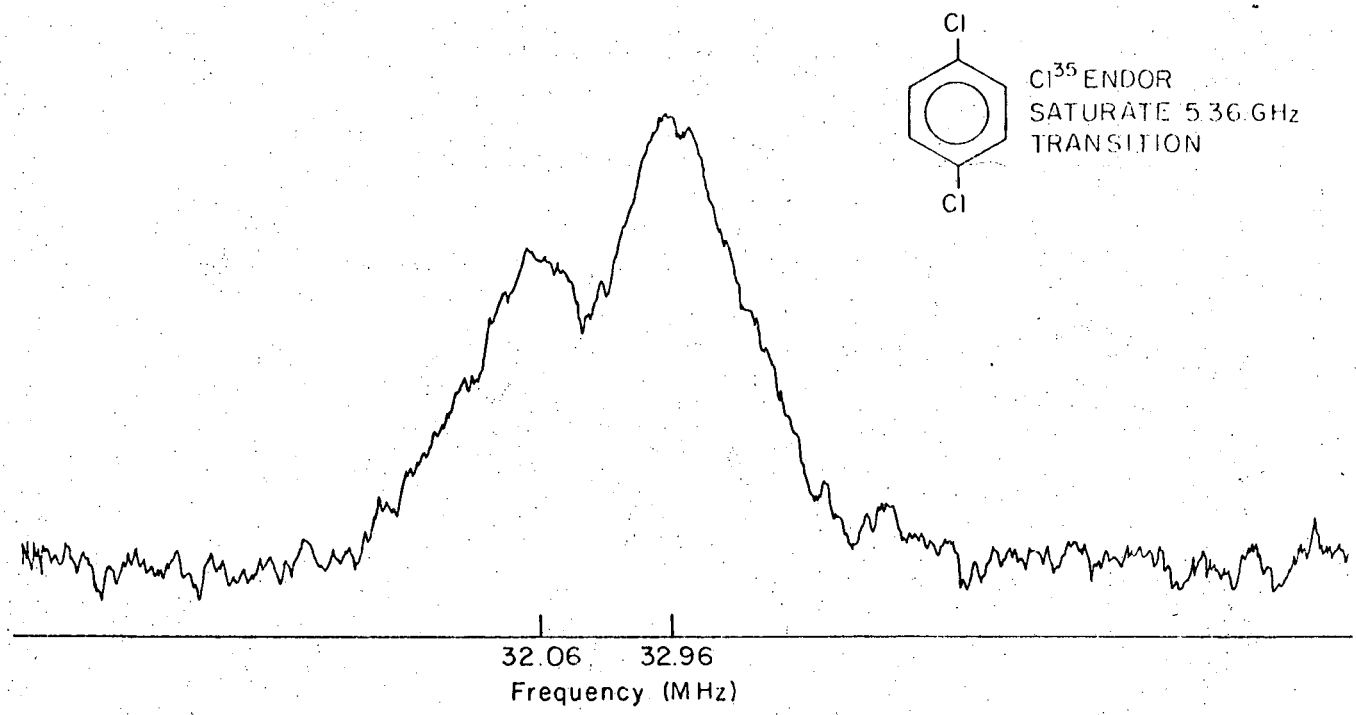

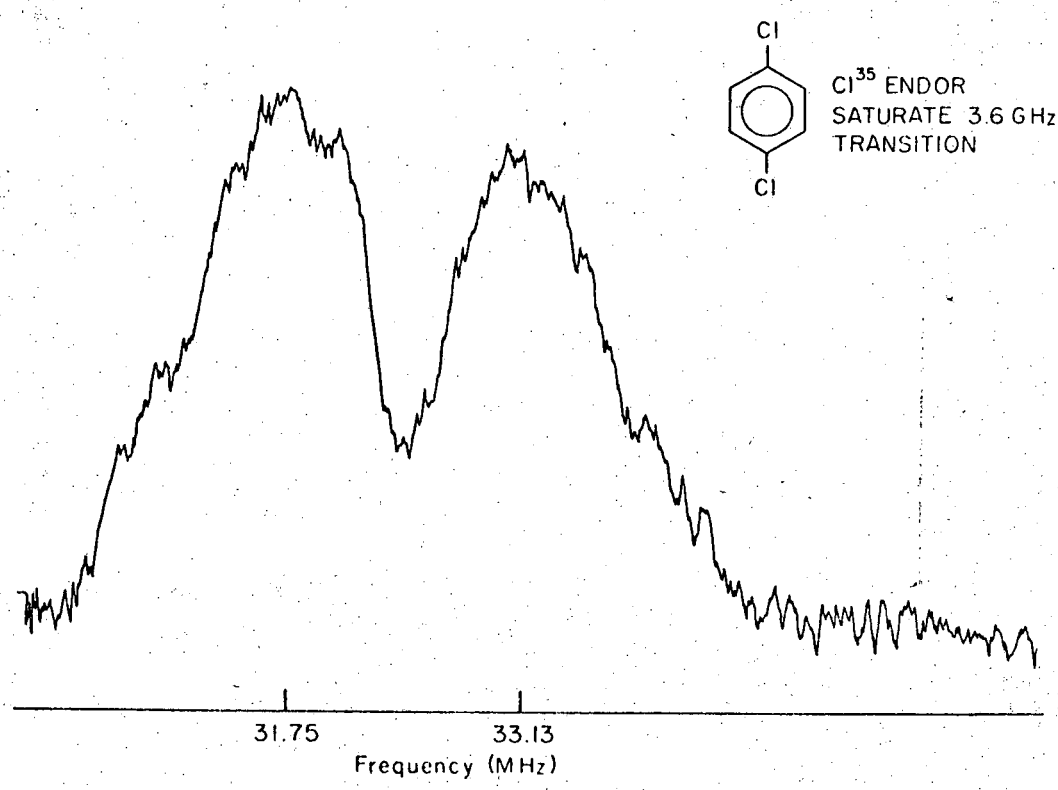

Fig. 4

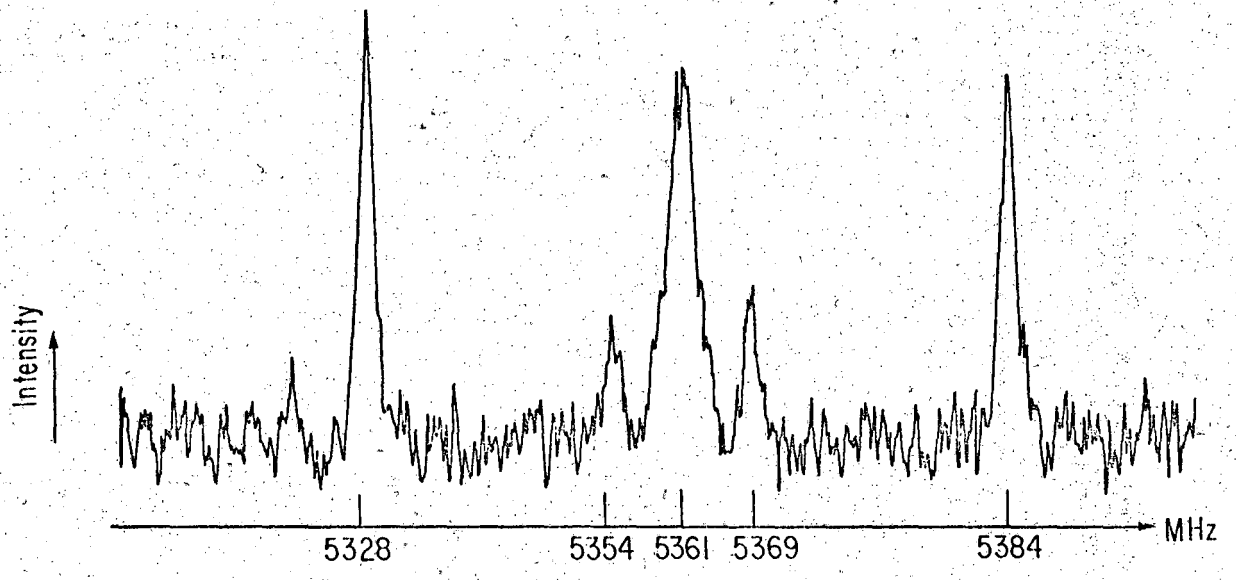

XBL 7012-7280

Fig. 5

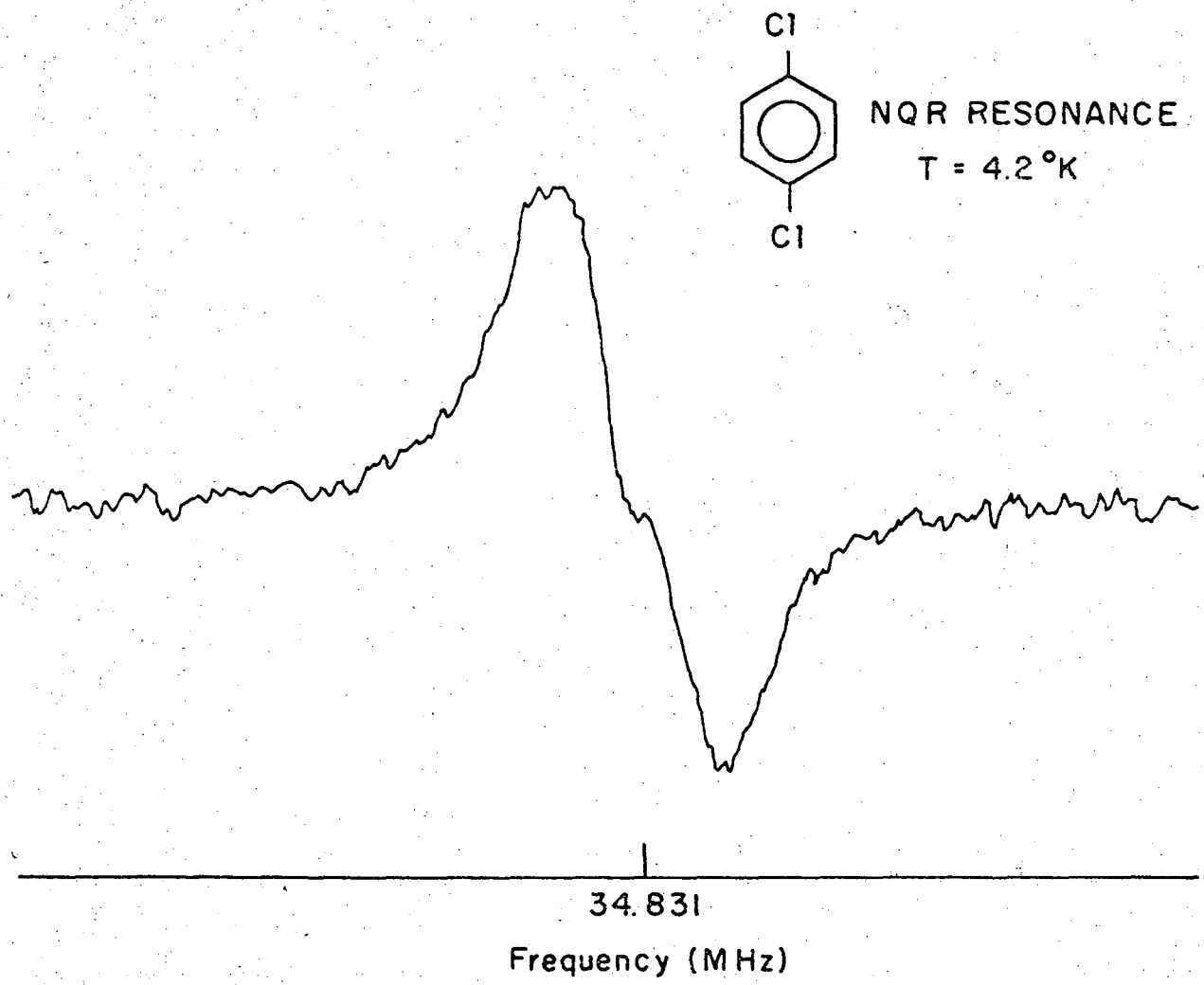

Fig. 6

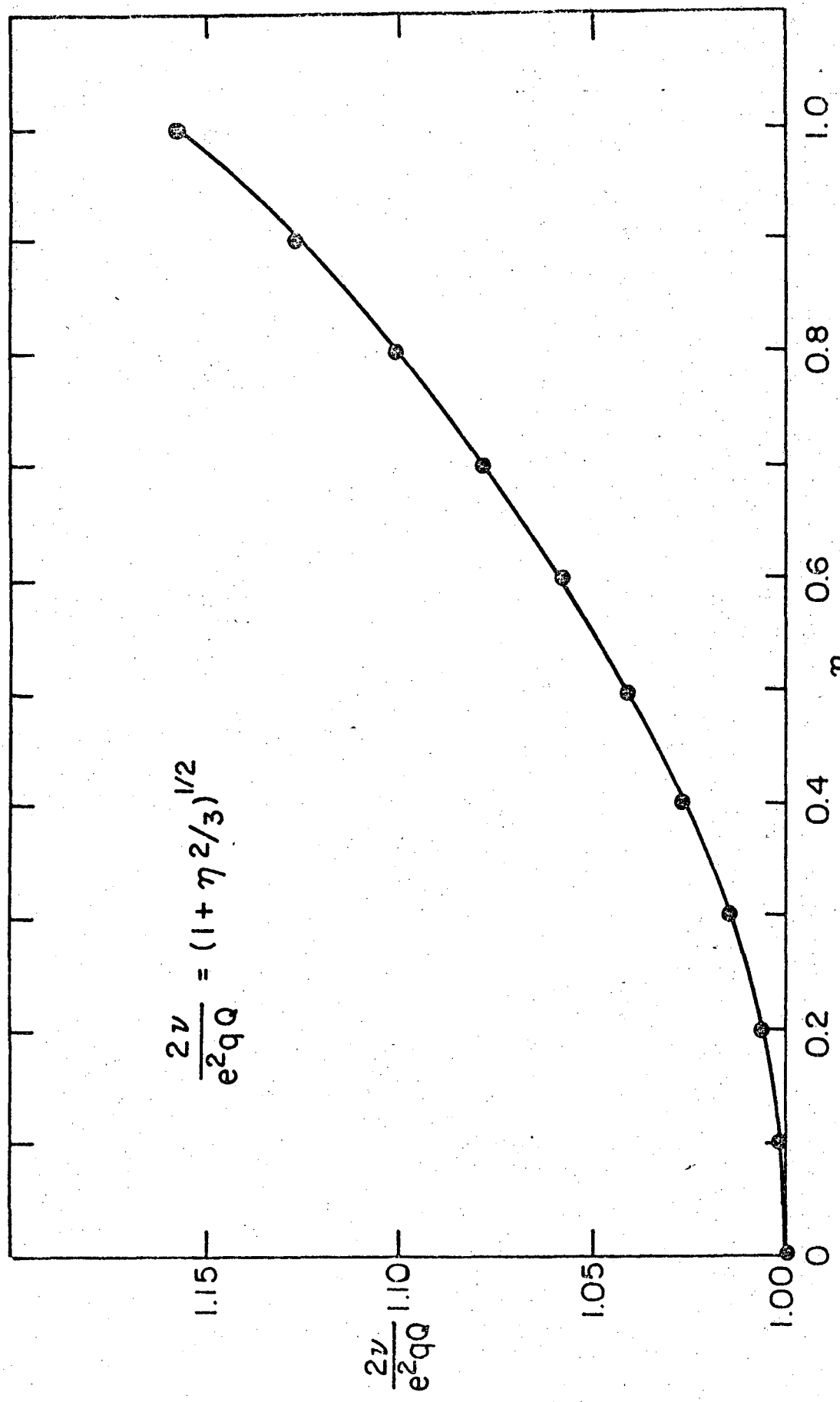
$\frac{2\nu}{e^2qQ} = (1+\eta^{2/3})^{1/2}$
$\frac{2\nu}{e^2qQ}$
1.15
1.10
1.05
1.00
0
0.2
0.4
0.6
0.8
1.0
η

Fig. 7

Figure Captions

Figure 1 Experimental arrangement for optically detected ESR in zero magnetic field.

Figure 2 Experimental arrangement for optically detected ENDOR in zero magnetic field. An enlarged view of the sample and ENDOR coil schematic is shown on the left.

Figure 3 ODMR of the $\tau_x \rightarrow \tau_y$ multiplet of paradichlorobenzene.

Figure 4 ^{35}Cl ENDOR resonance associated with the $\tau_x \rightarrow \tau_y$ and $\tau_x \rightarrow \tau_z$ electron spin transitions.

Figure 5 ^{35}Cl ENDOR pumping of the $\tau_x \rightarrow \tau_y$ multiplet.

Figure 6 Pure NQR resonance of the ground state of DCB at 4.2°K.

Figure 7 Plot of the measured NQR transition frequency divided by the nuclear quadrupole coupling constant versus the asymmetry parameter (η).

ESR EXPERIMENT

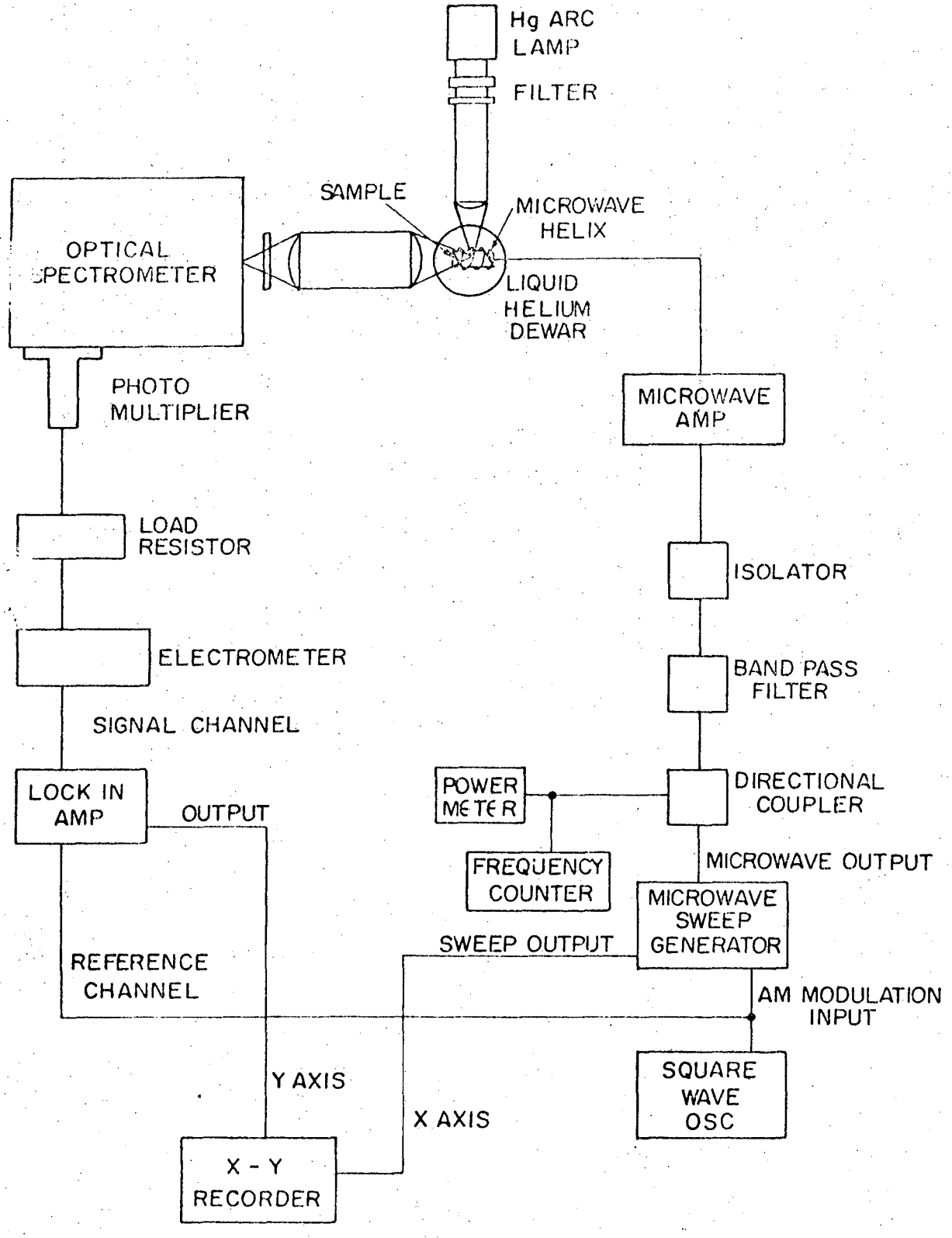

Fig. 1

TECHNICAL INFORMATION DIVISION
LAWRENCE BERKELEY LABORATORY
UNIVERSITY OF CALIFORNIA
BERKELEY, CALIFORNIA 94720